L-Type Amino Acid Transporters LAT1 and LAT4 in Cancer: Uptake of 3-*O*-Methyl-6-^{18}F-Fluoro-L-Dopa in Human Adenocarcinoma and Squamous Cell Carcinoma In Vitro and In Vivo

Cathleen Haase[1], Ralf Bergmann[1], Frank Fuechtner[1], Alexander Hoepping[2], and Jens Pietzsch[1]

[1]*Department of Radiopharmaceutical Biology, Institute of Radiopharmacy, Research Center Dresden–Rossendorf, Dresden, Germany; and* [2]*ABX Advanced Biochemical Compounds GmbH, Radeberg, Germany*

Expression of system L amino acid transporters (LAT) is strongly increased in many types of tumor cells. The purpose of this study was to demonstrate that ^{18}F-labeled amino acids, for example, 3-*O*-methyl-6-^{18}F-fluoro-L-dopa (^{18}F-OMFD), that accumulate in tumors via LAT represent an important class of imaging agents for visualization of tumors in vivo by PET. **Methods:** ^{18}F-OMFD uptake kinetics, transport inhibition, and system L messenger RNA expression were studied in vitro in human adenocarcinoma (HT-29), squamous cell carcinoma (FaDu), macrophages (THP-1), and primary aortic endothelial cells (HAEC) and in vivo in the corresponding mouse tumor xenograft models. **Results:** Uptake of ^{18}F-OMFD in all cell lines tested was mediated mainly by the sodium-independent high-capacity LAT. We found higher uptake in FaDu cells (V_{max}, 10.6 ± 1.1 nmol/min × mg of cell protein) and in the corresponding FaDu tumor xenografts than in the other cells and corresponding xenograft models studied. Quantitative messenger RNA analysis revealed that tumor cells and xenografts have a higher expression of LAT1 than do HAEC and THP-1 macrophages. However, only in the FaDu tumor model did an increased ^{18}F-OMFD uptake seem to be explained by increased LAT expression. Furthermore, we demonstrated a high expression of LAT4, a recently identified LAT. **Conclusion:** Our findings support the hypothesis that ^{18}F-OMFD is a tracer for visualization of tumor cells. ^{18}F-OMFD particularly seems to be a suitable tracer for diagnostic imaging of amino acid transport in poorly differentiated squamous cell head and neck carcinoma with increased LAT1 and LAT4 expression.

Key Words: L-type amino acid transporters; tumor cell lines; tumor xenograft models; monocyte/macrophage cell line; primary aortic endothelial cells

J Nucl Med 2007; 48:2063–2071
DOI: 10.2967/jnumed.107.043620

PET is an excellent technique for examining various biochemical processes in malignant tissues in vivo—for example, enhanced glycolysis, altered protein synthesis rates, and enhanced amino acid transport—by applying certain radiotracers (*1*). Tumor visualization with the most common tracer, ^{18}F-FDG, often is disturbed because of the high uptake of ^{18}F-FDG in nonmalignant tissues, such as the brain or inflammatory lesions. In contrast to ^{18}F-FDG uptake, uptake of amino acid tracers in macrophages and other inflammatory cells is thought to be low; thus, ^{18}F-labeled amino acids appear to be a promising class of more specific tumor-imaging agents (*2*). In this context, radiolabeled amino acids have been proved to be particularly useful for the imaging of brain tumors but also of peripheral tumors such as lymphoma, lung tumors, and breast tumors (*3–5*).

3-*O*-methyl-6-^{18}F-fluoro-L-DOPA (^{18}F-OMFD), a phenylalanine derivative, is a suitable ^{18}F-labeled amino acid analog for tumor imaging (*6–8*). This amino acid tracer offers the opportunity to study system L amino acid transporters (LATs) of human cancer in vivo with PET. Previous publications have indicated that system L is also present in microvascular endothelial cells of the human brain and plays an important role in the absorption of amino acids (*9*). Furthermore, interaction between tumor cells and endothelial cells is an essential component in the transition of tumors from a dormant state to a malignant state, because angiogenesis plays a key role in carcinogenesis (*10*).

Several transporters with system L characteristics have been identified at the molecular level. The first cloned transporters with system L activity were LAT1 and LAT2, which are members of the solute carrier 7 family of transporters (*11,12*). They mediate sodium-independent amino acid exchange and recognize a wide range of large neutral amino acids as substrates (*13*), expanding to small neutral amino acids in the case of LAT2 (*14*). LAT1 and LAT2 form heteromeric complexes via a disulfide bond with the heavy chain of 4F2 antigen (4F2hc, solute carrier 3A2), a single

Received May 14, 2007; revision accepted Aug. 23, 2007.
For correspondence or reprints contact: Cathleen Haase, PhD, Department of Radiopharmaceutical Biology, Institute of Radiopharmacy, Research Center Dresden–Rossendorf, P.O. Box 51 01 19, 01314 Dresden, Germany.
E-mail: c.haase@fzd.de

transmembrane domain protein essential for the functional expression of LAT1 and LAT2 at the plasma membrane (*15,16*). Recently, LAT3 (solute carrier 43) was identified, and several properties distinguish LAT3 from LAT1 and LAT2. For example, LAT3 does not require coexpression with 4F2hc and further exhibits a narrow substrate selectivity, preferring phenylalanine to others as substrates (*17*). Recently, LAT4 (solute carrier 43) was shown to have transport activity similar to that of LAT3 but a different tissue distribution (*17*). LAT1 is supposed to be the only transporter that plays an important role in cell proliferation and shows increased transport activity in many cancer cells (*18,19*).

The aim of the present study was to investigate the main transport system for uptake of the amino acid tracer ^{18}F-OMFD in different cells: human colorectal adenocarcinoma cells (HT-29), human head and neck squamous cell carcinoma cells (FaDu), and primary human aortic endothelial cells (HAEC). For differentiation of concomitant tracer uptake in tumor and inflammatory cells, we used a phorbol ester–stimulated human monocyte/macrophage cell line (THP-1), which represents a well-characterized model for proinflammatory cells and tissue-associated macrophages, respectively. We further studied ^{18}F-OMFD uptake in the corresponding tumor (HT-29 and FaDu) xenograft models in nude mice in vivo.

Using quantitative reverse transcription (RT) polymerase chain reaction (PCR), we characterized the expression of messenger RNA (mRNA) in the LAT1, LAT2, LAT3, LAT4, and 4F2hc subtypes.

MATERIALS AND METHODS

Cell Culture

Human aortic endothelial cells (HAEC) were obtained from Cascade Biologics and cultivated in EC medium MV2 (Promocell). Human tumor cell lines FaDu (head and neck squamous cell carcinoma) (American Type Culture Collection number HTB-43) and HT-29 (colorectal adenocarcinoma) (American Type Culture Collection number HTB-38) were obtained from DSMZ and cultivated in McCoy medium (FaDu) and RPMI (HT-29) supplemented with 10% fetal calf serum. THP-1 cells (European Collection of Cell Cultures number 88081201; human monocyte/macrophage cell line, stimulated with phorbol myristate acetate [64 nmol/L] for 72 h) were cultivated in RPMI with 10% fetal calf serum. All media and supplements were obtained from Biochrom. Cells were cultivated with 5% CO_2 and 37°C in a CO_2 incubator (Heracell; Heraeus).

RNA Isolation

For preparation of total RNA from cells and xenograft tumors, the Perfect RNA Mini Kit (Eppendorf) was used according to the manufacturer's recommendations.

Real-Time PCR

RT was done with a 2-step cMaster RT Kit (Eppendorf) according to the manufacturer's instructions.

SYBR GREEN I (1:30, 000) (Sigma) real-time PCR assay was performed in a 20-μL PCR mixture volume consisting of SYBR GREEN I in ×10 HotMaster Taq buffer (Eppendorf), $MgCl_2$ (2.5 mmol/L), the primers (200 nmol of each per liter), deoxyribonucleoside triphosphate (250 μmol/L), HotMaster Taq DNA polymerase (2.5 U), and cMaster RT reaction (5 μL). After amplification, the melting curve was analyzed to detect the correct product by its specific melting temperature and to verify the specificity of the amplicons. All PCR products were analyzed by agarose gel electrophoresis, and no unspecific PCR bands were detected. All primers (Table 1) were designed from their complementary DNA (LAT1 accession number, AB018009; LAT2 accession number, AB037669; LAT3 accession number, AB103033; LAT4 accession number, BC027923; 4F2hc accession number, AB018010; ASC1 accession number, NM_003038; ASC2 accession number, NM_005628; and 18S ribosomal RNA (rRNA) accession number, X03205) (http://frodo.wi.mit.edu/cgi-bin/primer3/primer3_www.cgi) and synthesized by Metabion. For each gene, 6 individual RNA samples

TABLE 1
Sequences of Primers used in RT-PCR

Complementary DNA	Primer sequence (5′to 3′)	Binding site	Product length	Annealing
LAT-1	AGGAGCCTTCCTTTCTCCTG	s 1,948–1,967	181 bp	60°C
LAT-1	CTGCAAACCCTAAGGCAGAG	as 2,109–2,128		60°C
LAT-2	ACCGAAACAACACCGAAAAG	s 729–748	155 bp	60°C
LAT-2	GATTCCAGAGCCGATGATGT	as 864–883		60°C
LAT-3	GCTGTGCTGGAGAACCTCTT	s 71–90	209 bp	60°C
LAT-3	CTGAGCACGAAGGAACCAAT	as 260–279		60°C
LAT-4	TCTCTCCGTGCTCATCTTCA	s 2–19	165 bp	60°C
LAT-4	ATTCCTGGAAAGGTGACTGC	as 147–166		60°C
4F2hc	TCTTGATTGCGGGGACTAAC	s 932–951	195 bp	60°C
4F2hc	GCCTTGCCTGAGACAAACTC	as 1,107–1,126		60°C
ASC-1	CCTACTTTGGCCTCACCACA	s 360–379	195 bp	60°C
ASC-1	CAAGATTGGAGGGAAACAGG	as 535–554		60°C
ASC-2	ACATCCTGGGCTTGGTAGTG	s 32–51	213 bp	60°C
ASC-2	GGGCAAAGAGTAAACCCACA	as 225–244		60°C
18S rRNA	CGGCTACCACATCCAAGGAAG	s 450–471	188 bp	65°C
18S rRNA	GCTGGAATTACCGCGGCTGCT	as 616–636		65°C

s = sense; as = antisense.

from each cell line were analyzed in a dual assay. The threshold cycle, which records the cycle when sample fluorescence exceeds a chosen threshold above background fluorescence, was divided through the threshold cycle of the internal 18S rRNA housekeeping gene, and the quotient was termed the relative expression level.

^{18}F-OMFD Synthesis

The amino acid derivative ^{18}F-OMFD (Scheme 1) was synthesized by direct electrophilic radiofluorination via stereoselective destannylation of the precursor *N*-formyl-3-*O*-methyl-4-*O*-boc-6-trimethylstannyl-L-DOPA-ethyl ester as published previously (*6*). In the present study, the radiochemical purity was more than 98% and the specific activity was 27.4 ± 2.1 GBq/mmol if 1.5 GBq of ^{18}F-OMFD were synthesized.

Uptake Experiments

The ^{18}F-OMFD (2 MBq/mL) cell tracer uptake experiments were performed in RPMI medium and phosphate-buffered saline (PBS) supplemented with glucose (11.1 mmol/L) at 4°C and 37°C for 0.5, 1, 2, 3, 5, 10, and 15 min. After the tracer uptake was stopped with 1 mL of ice-cold PBS, the cells were washed 3 times with PBS and dissolved in 0.5 mL of a 0.1 mol/L concentration of NaOH plus 1% sodium dodecylsulfate. The radioactivity in the cells was measured with a Cobra II γ-counter (Canberra-Packard). The total protein concentration in the samples was determined by the bicinchoninic acid method (Pierce). The energy dependence of tracer uptake was characterized by comparing the uptake kinetics of ^{18}F-OMFD at both 4°C and 37°C or in experiments using 15 mmol of sodium azide (NaN_3) per liter.

Competitive Inhibition Experiments

To characterize the transport system, we performed the inhibition experiments with specific competitive inhibitors: 2-aminobicyclo(2.2.1)heptane-2-carboxylic acid (BCH) for system L, α-(methylamino)isobutyric acid (MeAIB) for system A, and serine for system ASC using different concentrations (respectively, 0.15, 1.5, and 15 mmol/L). The cells were incubated with ^{18}F-OMFD (2 MBq/mL) and the specific inhibitors at 37°C for 2, 5, 10, and 15 min. The radioactivity and protein concentrations were measured as described above.

Animal Model

Animal experiments were performed on an established mouse tumor xenograft model (NMRI *nu/nu* male mice, with HT-29 and FaDu tumor implanted; $n = 3$) according to the guidelines of the German Regulations for Animal Welfare. The protocol was approved by the local Ethical Committee for Animal Experiments. The nude mice were further immunosuppressed through whole-body irradiation with 4 Gy (200 kV of x-rays, 0.5-mm copper filter, 1 Gy/min) 2 d before tumor transplantation. According to a standardized protocol, a stock of cryoconserved tumor pieces was established for both tumor cell lines. Xenografts were initially established by subcutaneous implantation of 10^6 cells from cultured individual cell lines and passed several generations by transplantation of approximately 50 mg of nonnecrotic tumor tissues. For the experiments, source tumors were generated from this stock, cut into small pieces (50 mg), and transplanted subcutaneously into the right hind leg of intraperitoneally anesthetized mice (per kilogram of body weight, 120 mg of ketamine and 16 mg of xylazine (*20*)). When the tumors reached about 200 mg, imaging studies were performed on a dedicated small-animal PET scanner (microPET P4; CTI Concorde Microsystems). The animals were anesthetized through inhalation of desflurane 9% (v/v) (Suprane; Baxter) in 40% oxygen/air (gas flow, 1 L/min) and then were positioned and immobilized prone with their medial axis parallel to the axial axis of the scanner and their thorax, abdomen, and hind legs (organs of interest: pancreas and tumor) in the center of the field of view. For attenuation correction, a 15-min transmission scan was obtained using a rotating ^{57}Co point source before tracer injection and collection of the emission scans. Then, approximately 10 MBq of ^{18}F-OMFD were administered intravenously within 15 s in a 0.3-mL volume into a tail vein. Simultaneously with tracer application, PET was started for 60 min. Sinogram generation and image reconstruction followed the protocol given by us elsewhere (*21*). Three-dimensional tumor regions of interest were determined for the subsequent data analysis. As an index of ^{18}F-OMFD uptake in vivo, the maximum standardized uptake value at 60 min after injection was calculated in regions of interest for each PET measurement. This value, the ratio of ^{18}F-OMFD uptake in a tumor to the injected ^{18}F-OMFD activity normalized to body weight, was calculated using the Rover software package (ABX Radeberg).

Statistical Analysis

Descriptive data were expressed as means ± SDs. Differences between HT-29/FaDu tumor cells and the corresponding xenografts, HAEC endothelial cells, and THP-1 macrophages for gene expression and radiotracer uptake were assessed by univariate ANOVA with post hoc Bonferroni testing or the nonparametric Mann–Whitney *U* test. All data were analyzed using the SPSS statistical package (version 12.0 for Windows; SPSS Inc.). A value of *P* less than 0.05 was considered statistically significant.

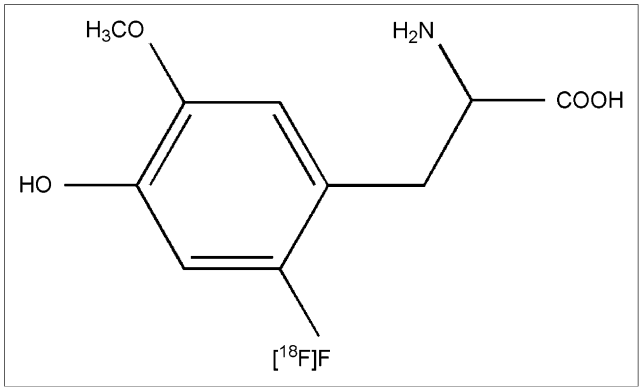

SCHEME 1. Chemical structure of ^{18}F-OMFD.

RESULTS

^{18}F-OMFD Uptake in FaDu Cells In Vitro

^{18}F-OMFD cellular uptake studies were performed either in RPMI or in PBS on the established human tumor cell lines FaDu and HT-29, on human endothelial cells HAEC, and on THP-1 macrophages. The tracer ^{18}F-OMFD was taken up quickly by all cells studied. Preliminary experiments studied the course of tracer uptake until 15 min (*7*). Therefore, in subsequent experiments, ^{18}F-OMFD uptake was assayed after 0.5, 1, 2, 5, 10, and 15 min. Figure 1 shows the kinetics of tracer uptake in RPMI and PBS in all cell lines. Uptake of ^{18}F-OMFD was significantly increased in FaDu cells, compared with all other cell lines,

for both PBS and RPMI (Fig. 1). Accumulated activity in FaDu cells was 5- to 10-fold higher for PBS than for RPMI (14% injected dose [%ID]/mg of protein) and reached 135 %ID/mg of protein. FaDu cells had already revealed an increased uptake (5.7-fold) after 5 min, compared with all other cell lines (Fig. 1). No significant differences were seen between tracer uptake of HT-29, HAEC, and THP-1 macrophages in RPMI or PBS. The average accumulated activity in these cells was about 3 %ID/mg of protein in RPMI and 35 %ID/mg of protein in PBS after 15 min.

To study the energy dependence of the observed ^{18}F-OMFD transport process, we compared uptake at 37°C with that at 4°C with and without adding 15 mmol of BCH per liter. No significant differences were found in any cell line. Furthermore, oxidative phosphorylation was inhibited by adding a 15 mmol/L concentration of NaN_3, which mimics the effects of hypoxia under normoxic conditions. However, NaN_3 did not significantly influence the uptake kinetics in any cell line.

Kinetics of ^{18}F-OMFD Uptake

To compare the functional expression of the L-amino transport systems in HT-29 and FaDu, as well as in differentiated THP-1 macrophages and primary HAEC, we studied the kinetics of ^{18}F-OMFD uptake. Uptake of ^{18}F-OMFD was measured in the presence of various concentrations of unlabeled OMFD. Uptake of ^{18}F-OMFD in all cell types studied was saturable and apparently followed Michaelis–Menton kinetics, with the K_m and V_{max} values given in Table 2. The maximum velocity of ^{18}F-OMFD uptake (V_{max}) was 10.6 ± 1.1 nmol/min × mg of cell protein and approximately 5-fold higher than in HT-29 cells, THP-1 macrophages, and HAEC.

Inhibition of ^{18}F-OMFD Uptake

To characterize the specificity of competitive inhibitors of the ^{18}F-OMFD transport system, we used BCH, MeAiB, and serine to inhibit the main transport systems L, A, and ASC, respectively. Inhibition experiments in PBS with different concentrations (0.15, 1.5, and 15 mmol/L) and at different times (5, 10, and 15 min) showed the same extent of tracer uptake and were almost identical for all cell lines studied (FaDu, HT-29, HAEC, and THP-1 macrophages). Figure 2 shows an example of ^{18}F-OMFD uptake after competitive inhibition in the FaDu cell line. In the presence of BCH, tracer uptake was significantly decreased—by approximately 90%—in all cell lines studied, compared with controls (Fig. 2A). Serine also caused a significant reduction in ^{18}F-OMFD uptake (Fig. 2B). MeAIB did not inhibit tracer uptake in any of the investigated cells (Fig. 2C). It appears, therefore, that most ^{18}F-OMFD uptake into cells was driven by systems L and ASC.

An additional experiment was conducted to analyze whether uptake of ^{18}F-OMFD in RPMI medium with amino acid concentrations corresponding to human plasma amino acid levels could also be completely inhibited by BCH and serine, compared with PBS supplemented only with glucose. Competitive inhibition experiments were done with serine (15 mmol/L), either alone or in combination with BCH (15 mmol/L), and uptake of ^{18}F-OMFD was measured after 2, 5, 10, and 15 min. Figure 3 shows an example of uptake inhibition in the FaDu cell line. Blocking with serine, either alone or in combination with BCH, significantly inhibited tracer uptake (Fig. 3A). After 15 min, 96% of the uptake was inhibited in serine-containing PBS and 98% in serine/BCH-containing PBS. Compared with PBS, RPMI medium showed a greater inhibition of ^{18}F-OMFD

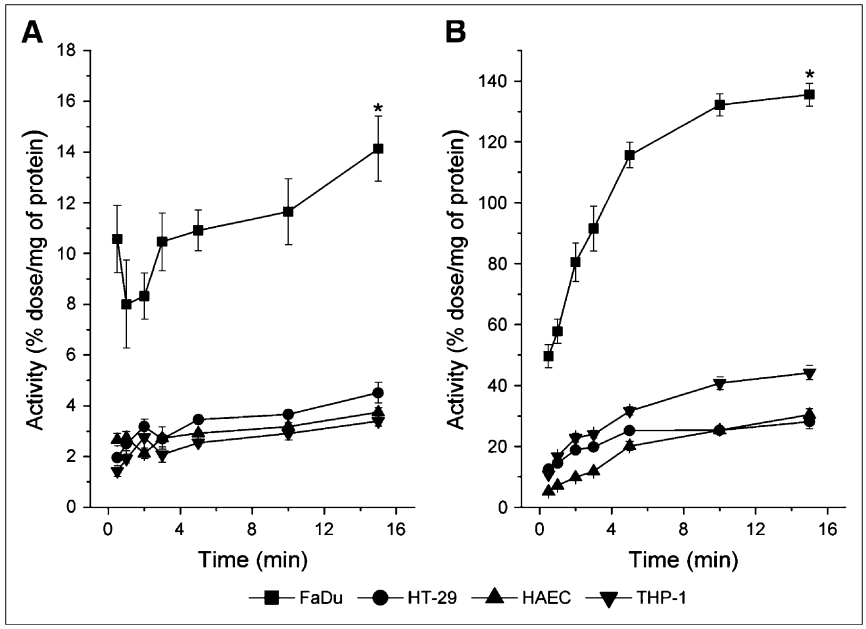

FIGURE 1. Time course of ^{18}F-OMFD (2 MBq/mL) uptake into tumor cells (HT-29, FaDu), endothelial cells (HAEC), and THP-1 macrophages after 0.5, 2, 5, 10, and 15 min measured in RPMI medium with amino acid concentrations corresponding to human plasma amino acid levels (A), compared with PBS supplemented with glucose (B). Data are mean ± SD (n = 15). *$P < 0.05$.

TABLE 2
Kinetic Parameters of ^{18}F-OMFD Uptake

Cell type	K_m (μmol/L)	V_{max} (nmol/min × mg of cell protein)
FaDu	85.8 ± 15.9	10.58 ± 1.14
HT-29	53.3 ± 5.2	2.07 ± 0.04
THP-1 macrophages	109.3 ± 16.9	2.68 ± 0.06
HAEC	126.8 ± 11.3	2.91 ± 0.09

uptake—63% for serine alone and 79% for serine/BCH (Fig. 3B).

Quantitative mRNA Expression of LAT1, LAT2, LAT3, LAT4, and 4F2hc (CD98)

We further examined the quantitative mRNA expression of LAT1, LAT2, LAT3, LAT4, and 4F2hc in these tumor cells (HT-29 and FaDu), in the corresponding tumor xenografts (HT-29 and FaDu), in endothelial cells (HAEC), and in THP-1 macrophages using quantitative real-time PCR. The data show that all investigated cells expressed LAT4, LAT1, and the associated protein 4F2hc (Fig. 4). The expression level of LAT4 detected both in the tumor cells and in the corresponding xenografts (Fig. 4) was significantly higher than that in the HAEC and THP-1 macrophages. The amount of LAT1 was found to be the same, compared with 4F2hc. Only HT-29 tumor cells revealed an increased amount of 4F2hc. FaDu cells and HT-29/FaDu xenografts showed an increased LAT1 expression level, compared with HT-29 and HAEC cells and THP-1 macrophages. LAT2 was detected only in THP-1 macrophages and showed no differences from LAT1, LAT4, and 4F2hc in expression level (Fig. 4). LAT3 expression could not be verified in any investigated cells. In the context of competitive inhibition of ^{18}F-OMFD uptake by serine, we furthermore performed quantitative real-time PCR for the 2 ASC transporter subtypes, ASC1 and ASC2, in all cells. We found a low expression level for ASC1 and ASC2, comparable to the expression level of LAT4 in HAEC and THP-1 macrophages.

^{18}F-OMFD Uptake in FaDu Xenografts In Vivo

Figure 5 shows a representative PET image of a mouse FaDu xenograft model after intravenous application of ^{18}F-OMFD. The highest radioactivity concentration was observed in the tumor and pancreas. Similar results were obtained in HT-29 xenograft models. However, ^{18}F-OMFD uptake was significantly higher in FaDu than in HT-29 (mean maximum standardized uptake value, 3.07 ± 0.66 (FaDu) vs. 1.19 ± 0.26 (HT-29); $P < 0.05$).

DISCUSSION

In the present study, we investigated both amino acid uptake transport of ^{18}F-OMFD and expression of the amino acid transport systems in 2 different tumor cell lines (HT-29 and FaDu), in the corresponding mouse tumor xenograft models, and in primary endothelial cells (HAEC) and THP-1 macrophages to evaluate L-system transporters as specific targets for tumor visualization using ^{18}F-labeled amino acids.

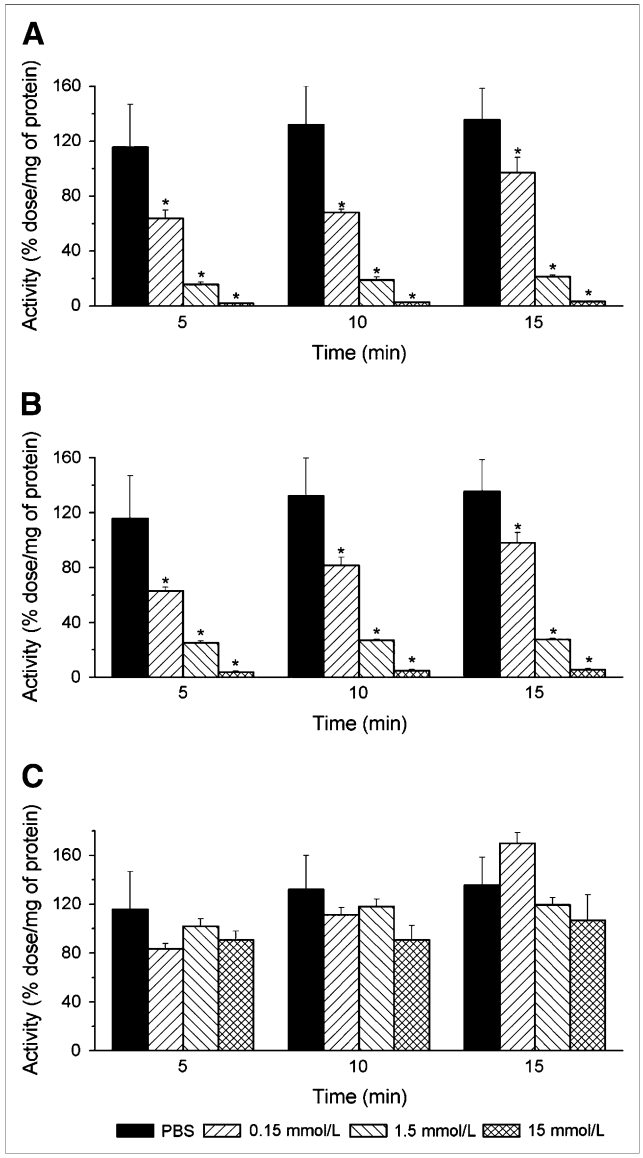

FIGURE 2. ^{18}F-OMFD (2 MBq/mL) uptake into FaDu tumor cells at different times (5, 10, and 15 min) after incubation with different concentrations (0.15, 1.5, and 15 mmol/L) of specific transport inhibitors: BCH for system L (A), serine for system ASC (B), and MeAIB for system A (C). Data are mean ± SD (n = 10). *$P < 0.05$.

Amino acid transport tracers are amino acids that are transported into the cells and do not actually participate in protein synthesis (*22*), examples being *O*-^{18}F-fluoromethyl-L-tyrosine (*23*), *O*-2-^{18}F-fluoroethyl-L-tyrosine (*24*), and ^{18}F-OMFD (*7*). In the past, ^{18}F-OMFD was considered mainly as a metabolite of 6-^{18}F-fluoro-L-3,4-dihydroxyphenylalanine that is able to pass the blood–brain barrier, thereby contributing to ^{18}F uptake in the striatum. Therefore,

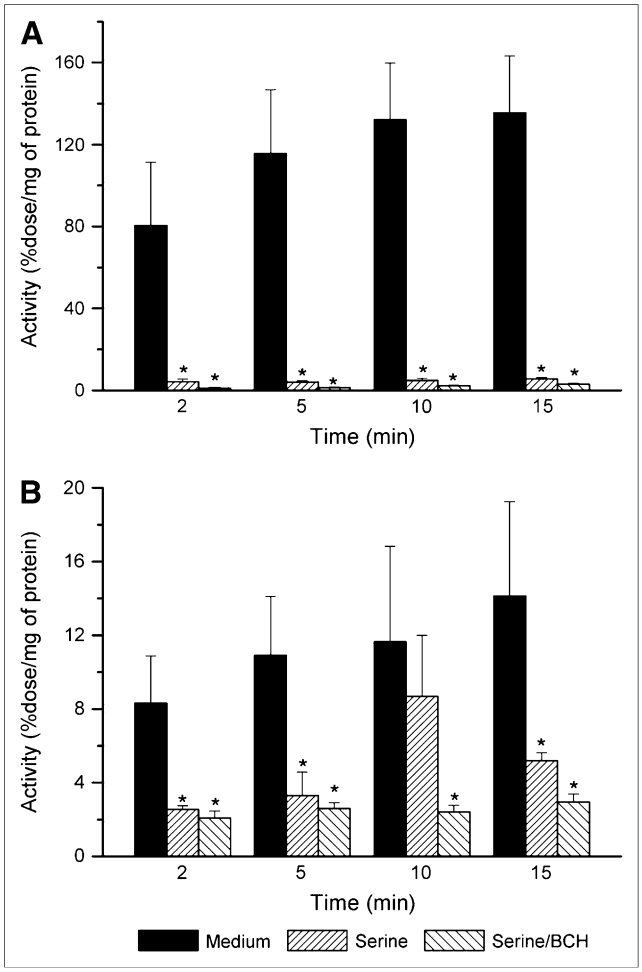

FIGURE 3. ^{18}F-OMFD (2 MBq/mL) uptake into FaDu tumor cells after incubation with serine (15 mmol/L) and in combination with BCH (15 mmol/L) in PBS with glucose (A) and RPMI medium with amino acid concentrations corresponding to human plasma amino acid levels (B) at different times (2, 5, 10, and 15 min). Data are mean ± SD (n = 10). *$P < 0.05$.

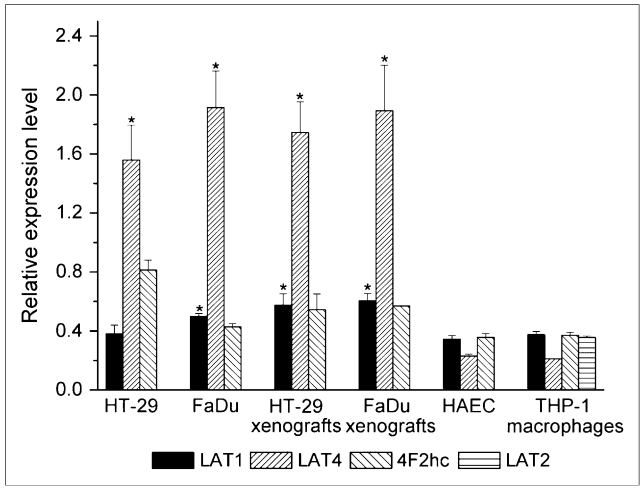

FIGURE 4. LAT1, LAT2, LAT4, and 4F2hc mRNA expression studies in HT-29 and FaDu tumor cells and corresponding xenografts, HAEC endothelial cells, and THP-1 macrophages using quantitative real-time PCR. Arithmetic chart of threshold cycle for LAT1, LAT2, LAT4, and 4F2hc was normalized to housekeeping gene 18S-rRNA expression. Data are mean ± SD (n = 8). *$P < 0.05$.

it has to be considered for the formulation of a quantitative 6-^{18}F-fluoro-L-3,4-dihydroxyphenylalanine kinetic model (*25*). ^{18}F-OMFD, a methoxy derivative of the amino acid tracer 2-^{18}F-fluoro-L-tyrosine (*26*), is supposed to be a promising PET tracer for imaging the functional expression of amino acid transport systems in tumors.

Various specific transport systems for amino acids have been characterized in mammalian cells (*27,28*). For uptake of neutral amino acids, the main carrier systems are the A, L, and ASC systems. The A and ASC systems are sodium-dependent and mediate the uptake of neutral amino acids with short, polar, or linear side chains. System L activity is presently attributed to 4 Na^+-independent transporters called LAT1, LAT2, LAT3, and LAT4. LAT1 and LAT2 are catalytic 4F2 light chains, whereas LAT3 and LAT4 have been shown to function without 4F2hc (*17,29*). LAT1 is supposed to be the only transporter that plays an important role in cell proliferation and shows increased transport activity in many cancer cells (*15,18,30*). However, there have been only a few in vitro studies using fluorine-labeled amino acids on tumor cell lines (*7,31,32*). Moreover, in our study we analyzed, for what is to our knowledge the first time, fluorine-labeled amino acid uptake in a comparison of tumor cells with primary human aortic endothelial cells and macrophages, which represent model cells for tumor-associated endothelial cells and macrophages, respectively.

The cellular uptake studies demonstrated that ^{18}F-OMFD transport into the cells apparently followed Michaelis–Menton kinetics and was saturable by the transported substrate. The cells used in our experiments strongly differ in their extent of transformation and degree of differentiation. It is thought that besides influencing physiologic functions, these differences also influence amino acid transport processes, thus in part explaining the different tracer uptake velocities in the cells.

The 2 different tumor cell lines, FaDu and HT-29, significantly differ in regulation of their cell cycles and in growth properties. FaDu, a poorly differentiated head and neck squamous cell carcinoma, has a shorter doubling time (2.8–3.0 d) than HT-29 (3.5 d), a moderately differentiated colon carcinoma (*33*).

FaDu shows significant high ^{18}F-OMFD uptake both in cell lines in vitro and in the corresponding xenografts in vivo. In FaDu cells, V_{max} was higher by a factor of 5 and the affinity of ^{18}F-OMFD to the transport system (K_m) was 1.6 times lower than in HT-29 cells, confirming our former data (*7*). As a new finding, THP-1 macrophages and HAEC showed a low V_{max} similar to that of HT-29 cells but a 2 times lower affinity to the transport system (K_m) for ^{18}F-OMFD than for HT-29. However, only in the FaDu tumor model did increased ^{18}F-OMFD uptake seem to be

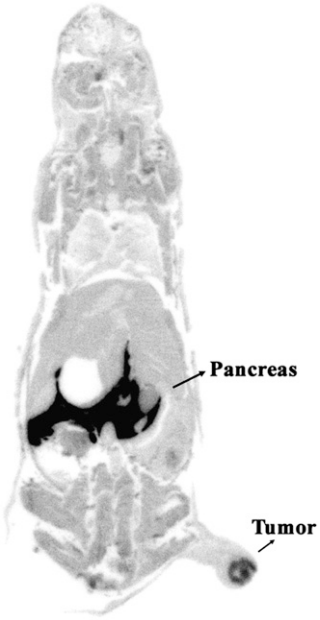

FIGURE 5. Representative small-animal PET image (maximum intensity projection) of mouse tumor (FaDu) xenograft model after intravenous administration of 10 MBq of ^{18}F-OMFD (60 min after injection).

explained by increased LAT1 mRNA expression. With respect to this discrepancy observed between tracer uptake experiments and quantitative mRNA analysis of amino acid transporter expression, one needs to consider that quantitative expression on the mRNA level does not fully reflect the levels of total active transport proteins or the quantitative percentage of each transporter subtype on the cell membrane surface. A systematic Western blot analysis has not been performed, because specific antibodies are not yet available for all amino acid transport proteins of interest. Considering this constraint of the present study, however, the total number of transporters can be higher in FaDu cells than in HT-29 cells although showing a comparable mRNA expression level (related to the housekeeping gene 18S rRNA). This fact is, in part, reflected by the K_m and V_{max} values stated in this article.

For competitive inhibition of the different amino acid transport systems, the following inhibitors were used: BCH for the L system, MeAIB for the A system, and serine for the ASC system. ^{18}F-OMFD uptake in all cells analyzed was inhibited by BCH and serine, whereas MeAIB did not have any inhibitory effect. Contrasting with our previous studies is the finding of a significant inhibition of ^{18}F-OMFD uptake by serine, although ^{18}F-OMFD uptake is sodium-independent (*7*). BCH is known to be a specific inhibitor of the sodium-independent L system (LAT1, LAT2, LAT3, and LAT4). Serine, on the other hand, is a specific inhibitor of the sodium-dependent ASC system (ASC1 and ASC2) (*34*). Actually, system ASC was designated as such for transporting alanine, serine, and cysteine and other small neutral amino acids (*35*). However, functional studies revealed a broader substrate selectivity for ASC1 than for ASC2—a selectivity that includes not only a high affinity for small neutral amino acids but also a low affinity for some long-chain amino acids, such as several LAT1 substrates (*36*). On the other hand, recent studies showed that LAT1 and LAT2 functioned also as transporters for serine (*37,38*). In some cell types, serine accumulation is predominantly mediated by LAT (*39*). Another study suggested that serine may inhibit LAT1 and LAT2 both in sodium-free and sodium-containing media (*40*). If only the LAT system were active in ^{18}F-OMFD transport, one would expect to find additional inhibition by serine under sodium-free conditions. Notably, for all uptake studies in the present study, we used only cell lines that were newly obtained from the respective supplier and were in passages 6 and 7. Long cultivation times are likely to cause genetic instability and variation, and moreover, contamination will change the individual properties of each cell line. In our previous studies, the use of cell lines with different and sometimes long passages could be a reason for the different behavior in the blocking experiments with serine (*7*). Another explanation could be the enhanced specific activity of ^{18}F-OMFD—5-fold higher in the present study than in our previous study. On the basis of our results, we suppose that ^{18}F-OMFD uptake is mediated mainly by system L. Considering the sodium dependence of the ASC system, a contribution from the ASC system to the overall uptake of ^{18}F-OMFD cannot be assumed. Moreover, the expression level of ASC1 and ASC2 is low in all cell lines.

Preclinical experiments aiming at tumor-specific uptake of ^{18}F-OMFD using in vivo small-animal PET partly confirmed the in vitro results by showing a significantly higher ^{18}F-OMFD uptake (maximum standardized uptake value) in FaDu tumor xenografts than in HT-29 tumor xenografts.

Of particular interest was the high ^{18}F-OMFD uptake observed in the pancreas. This high uptake, like that of other amino acid tracers, such as *O*-2-^{18}F-fluoroethyl-L-tyrosine (*32*), is hypothesized to indicate high amino acid transport activity in this organ because of the increased amino acid requirement for synthesis of several hormones and enzymes.

All the investigated cells and tumor xenografts express LAT1, its associated protein 4F2hc, and LAT4, whereas FaDu cells and FaDu/HT-29 xenografts have a significantly higher expression of only LAT1.

We detected, for what is to our knowledge the first time, overexpression of LAT4 in tumor cells and xenografts; the overall expression was 3- to 4-fold higher than that of LAT1. As is already known, LAT1 is highly expressed in malignant tumors, presumably to support their continuous growth and proliferation (*41*). LAT4, a recently identified amino acid transporter with L activity (*17*), has not yet been well characterized and has not been implicated in tumor growth and proliferation. LAT4 has a narrow substrate selectivity, preferring leucine, isoleucine, and phenylalanine (*17*). Most efforts have focused on the cloning, characterizing, and classifying of this integral membrane protein,

whereas studies of the biologic utility are still ongoing. No evidence has suggested that LAT4 has a role in carcinogenesis.

Furthermore, we found LAT2 mRNA expression only in THP-1 macrophages, and we found no LAT2 transcripts in any of the tumor cells or corresponding xenografts. LAT2 is believed to function predominantly as an efflux pathway (*12*). Studies using real-time PCR and Western blot analysis have already shown that different tumor cells express LAT1 and its associated protein, 4F2hc, at high levels, but not LAT2 (*18,42*). The similarity in ^{18}F-OMFD uptake between THP-1 cells and the HT-29 tumor model, despite a significantly lower LAT4 expression in the former (expression of LAT1 is comparable), could, in addition, be explained by a compensatory uptake via LAT2 that is expressed in THP-1 cells. For HAEC, a difference from HT-29 cells in the quantitative percentage of transporter subtypes on the cell membrane surface can be assumed.

Based on our studies, the recently identified transporter LAT4 and the well known LAT1 seem to be an excellent and promising target for further studies on tumor diagnosis and molecular imaging. We showed here, for what is to our knowledge the first time, high expression of LAT4, and further investigations need to focus on this transporter subtype with respect to tumor proliferation and growth. This newly gained knowledge of the molecular mechanism involved in the transport of essential amino acids will amplify the potential of radiolabeled amino acids in the diagnosis of, for example, squamous cell head and neck cancer.

CONCLUSION

Because of high accumulation of ^{18}F-OMFD in FaDu cells and the corresponding xenografts, PET with ^{18}F-OMFD possibly has the potential to improve staging and detection of certain types of cancer, particularly of poorly differentiated squamous cell head and neck tumors. In addition, ^{18}F-OMFD may allow quantification of important cellular processes related to tumor proliferation in certain tumor entities, such as squamous cell head and neck cancer. However, further study is needed of, on the one hand, the contribution of endothelial cells and proinflammatory cells such as macrophages and, on the other hand, the role of different LAT subtypes in overall uptake of ^{18}F-OMFD in tumors and inflammatory lesions.

ACKNOWLEDGMENTS

This work was supported in part by the Federal Ministry for Education and Research (BMBF) (Sign 03/4021) and a grant from the European Union (Molecular Imaging for Biologically Optimized Cancer Therapy, BIOCARE, contract 505785). We thank Dr. Stefan Hamm (ABX) for providing the precursor for the ^{18}F-OMFD and the reference standard. The excellent technical help of Nicole Ewald, Mareike Barth, and Regina Herrlich is gratefully acknowledged. We thank Christina Schütze, Dorothee Pfitzmann, Katja Schumann, and the staff of the Experimental Centre of the Medical Faculty of the University of Technology Dresden for providing the tumor xenograft models. We also thank the staff of GMP laboratory at the Institute of Radiopharmacy for expert technical assistance in ^{18}F-OMFD synthesis and quality control. We are also grateful to Bettina Beuthien-Baumann, MD, for her expert advice and many stimulating discussions.

REFERENCES

1. Gambhir SS, Czernin J, Schwimmer J, Silverman DH, Coleman RE, Phelps ME. A tabulated summary of the FDG PET literature. *J Nucl Med.* 2001;42(suppl): 1–93.
2. Stober B, Tanase U, Herz M, Seidl C, Schwaiger M, Senekowitsch-Schmidtke R. Differentiation of tumour and inflammation: characterisation of [methyl-^{3}H] methionine (MET) and O-(2-[^{18}F]fluoroethyl)-L-tyrosine (FET) uptake in human tumour and inflammatory cells. *Eur J Nucl Med Mol Imaging.* 2006;33: 932–939.
3. Langen KJ, Ziemons K, Kiwit JC, et al. 3-[^{123}I]iodo-alpha-methyltyrosine and [methyl-^{11}C]-L-methionine uptake in cerebral gliomas: a comparative study using SPECT and PET. *J Nucl Med.* 1997;38:517–522.
4. Leskinen-Kallio S, Nagren K, Lehikoinen P, Ruotsalainen U, Joensuu H. Uptake of ^{11}C-methionine in breast cancer studied by PET: an association with the size of S-phase fraction. *Br J Cancer.* 1991;64:1121–1124.
5. Nettelbladt OS, Sundin AE, Valind SO, et al. Combined fluorine-18-FDG and carbon-11-methionine PET for diagnosis of tumors in lung and mediastinum. *J Nucl Med.* 1998;39:640–647.
6. Fuchtner F, Steinbach J. Efficient synthesis of the ^{18}F-labelled 3-O-methyl-6-[^{18}F]fluoro-L-DOPA. *Appl Radiat Isot.* 2003;58:575–578.
7. Bergmann R, Pietzsch J, Fuechtner F, et al. 3-O-methyl-6-^{18}F-fluoro-L-dopa, a new tumor imaging agent: investigation of transport mechanism in vitro. *J Nucl Med.* 2004;45:2116–2122.
8. Beuthien-Baumann B, Bredow J, Burchert W, et al. 3-O-methyl-6-[^{18}F]fluoro-L-DOPA and its evaluation in brain tumour imaging. *Eur J Nucl Med Mol Imaging.* 2003;30:1004–1008.
9. Umeki N, Fukasawa Y, Ohtsuki S, et al. mRNA expression and amino acid transport characteristics of cultured human brain microvascular endothelial cells (hBME). *Drug Metab Pharmacokinet.* 2002;17:367–373.
10. Naumov GN, Akslen LA, Folkman J. Role of angiogenesis in human tumor dormancy: animal models of the angiogenic switch. *Cell Cycle.* 2006;5:1779–1787.
11. Torrents D, Estevez R, Pineda M, et al. Identification and characterization of a membrane protein (y+L amino acid transporter-1) that associates with 4F2hc to encode the amino acid transport activity y+L: a candidate gene for lysinuric protein intolerance. *J Biol Chem.* 1998;273:32437–32445.
12. Verrey F. System L: heteromeric exchangers of large, neutral amino acids involved in directional transport. *Pflugers Arch.* 2003;445:529–533.
13. Uchino H, Kanai Y, Kim DK, et al. Transport of amino acid-related compounds mediated by L-type amino acid transporter 1 (LAT1): insights into the mechanisms of substrate recognition. *Mol Pharmacol.* 2002;61:729–737.
14. Rossier G, Meier C, Bauch C, et al. LAT2, a new basolateral 4F2hc/CD98-associated amino acid transporter of kidney and intestine. *J Biol Chem.* 1999;274: 34948–34954.
15. Lahoutte T, Caveliers V, Camargo SM, et al. SPECT and PET amino acid tracer influx via system L (h4F2hc-hLAT1) and its transstimulation. *J Nucl Med.* 2004; 45:1591–1596.
16. Campbell WA, Thompson NL. Overexpression of LAT1/CD98 light chain is sufficient to increase system L-amino acid transport activity in mouse hepatocytes but not fibroblasts. *J Biol Chem.* 2001;276:16877–16884.
17. Bodoy S, Martin L, Zorzano A, Palacin M, Estevez R, Bertran J. Identification of LAT4, a novel amino acid transporter with system L activity. *J Biol Chem.* 2005; 280:12002–12011.
18. Kim Do K, Kim IJ, Hwang S, et al. System L-amino acid transporters are differently expressed in rat astrocyte and C6 glioma cells. *Neurosci Res.* 2004;50: 437–446.
19. Kobayashi H, Ishii Y, Takayama T. Expression of L-type amino acid transporter 1 (LAT1) in esophageal carcinoma. *J Surg Oncol.* 2005;90:233–238.
20. Haase C, Bergmann R, Oswald J, Zips D, Pietzsch J. Neurotensin receptors in adeno- and squamous cell carcinoma. *Anticancer Res.* 2006;26:3527–3533.

21. Berndt M, Pietzsch J, Wuest F. Labeling of low-density lipoproteins using the ^{18}F-labeled thiol-reactive reagent N-[6-(4-[^{18}F]fluorobenzylidene)aminooxyhexyl] maleimide. *Nucl Med Biol.* 2007;34:5–15.
22. Jager PL, Vaalburg W, Pruim J, de Vries EG, Langen KJ, Piers DA. Radiolabeled amino acids: basic aspects and clinical applications in oncology. *J Nucl Med.* 2001;42:432–445.
23. Ishiwata K, Kawamura K, Wang WF, et al. Evaluation of O-[^{11}C]methyl-L-tyrosine and O-[^{18}F]fluoromethyl-L-tyrosine as tumor imaging tracers by PET. *Nucl Med Biol.* 2004;31:191–198.
24. Wester HJ, Herz M, Weber W, et al. Synthesis and radiopharmacology of O-(2-[^{18}F]fluoroethyl)-L-tyrosine for tumor imaging. *J Nucl Med.* 1999;40:205–212.
25. Brust P, Bauer R, Walter B, et al. Simultaneous measurement of [^{18}F]FDOPA metabolism and cerebral blood flow in newborn piglets. *Int J Dev Neurosci.* 1998;16:353–364.
26. Coenen HH, Kling P, Stocklin G. Cerebral metabolism of L-[2-^{18}F]fluorotyrosine, a new PET tracer of protein synthesis. *J Nucl Med.* 1989;30:1367–1372.
27. Segel GB, Woodlock TJ, Murant FG, Lichtman MA. Photoinhibition of 2-amino-2-carboxybicyclo[2,2,1]heptane transport by O-diazoacetyl-L-serine: an initial step in identifying the L-system amino acid transporter. *J Biol Chem.* 1989;264: 16399–16402.
28. Saier MH Jr, Daniels GA, Boerner P, Lin J. Neutral amino acid transport systems in animal cells: potential targets of oncogene action and regulators of cellular growth. *J Membr Biol.* 1988;104:1–20.
29. Babu E, Kanai Y, Chairoungdua A, et al. Identification of a novel system L amino acid transporter structurally distinct from heterodimeric amino acid transporters. *J Biol Chem.* 2003;278:43838–43845.
30. Yoon JH, Kim IJ, Kim H, et al. Amino acid transport system L is differently expressed in human normal oral keratinocytes and human oral cancer cells. *Cancer Lett.* 2005;222:237–245.
31. Langen KJ, Jarosch M, Muhlensiepen H, et al. Comparison of fluorotyrosines and methionine uptake in F98 rat gliomas. *Nucl Med Biol.* 2003;30:501–508.
32. Heiss P, Mayer S, Herz M, Wester HJ, Schwaiger M, Senekowitsch-Schmidtke R. Investigation of transport mechanism and uptake kinetics of O-(2-[^{18}F]fluoroethyl)-L-tyrosine in vitro and in vivo. *J Nucl Med.* 1999;40:1367–1373.
33. Azrak RG, Cao S, Slocum HK, et al. Therapeutic synergy between irinotecan and 5-fluorouracil against human tumor xenografts. *Clin Cancer Res.* 2004;10: 1121–1129.
34. Christensen HN, Handlogten ME, Lam I, Tager HS, Zand R. A bicyclic amino acid to improve discriminations among transport systems. *J Biol Chem.* 1969;244: 1510–1520.
35. Christensen HN, Liang M, Archer EG. A distinct Na+-requiring transport system for alanine, serine, cysteine, and similar amino acids. *J Biol Chem.* 1967; 242:5237–5246.
36. Fuchs BC, Bode BP. Amino acid transporters ASCT2 and LAT1 in cancer: partners in crime? *Semin Cancer Biol.* 2005;15:254–266.
37. Kanai Y, Segawa H, Miyamoto K, Uchino H, Takeda E, Endou H. Expression cloning and characterization of a transporter for large neutral amino acids activated by the heavy chain of 4F2 antigen (CD98). *J Biol Chem.* 1998;273:23629–23632.
38. Segawa H, Fukasawa Y, Miyamoto K, Takeda E, Endou H, Kanai Y. Identification and functional characterization of a Na+-independent neutral amino acid transporter with broad substrate selectivity. *J Biol Chem.* 1999;274:19745–19751.
39. Takarada T, Balcar VJ, Baba K, et al. Uptake of [^{3}H]L-serine in rat brain synaptosomal fractions. *Brain Res.* 2003;983:36–47.
40. Budy B, O'Neill R, DiBello PM, Sengupta S, Jacobsen DW. Homocysteine transport by human aortic endothelial cells: identification and properties of import systems. *Arch Biochem Biophys.* 2006;446:119–130.
41. Yanagida O, Kanai Y, Chairoungdua A, et al. Human L-type amino acid transporter 1 (LAT1): characterization of function and expression in tumor cell lines. *Biochim Biophys Acta.* 2001;1514:291–302.
42. Yoon JH, Kim YB, Kim MS, et al. Expression and functional characterization of the system L amino acid transporter in KB human oral epidermoid carcinoma cells. *Cancer Lett.* 2004;205:215–226.